Infrared Spectra and Density Functional Calculations for SMO_2 Molecules (M = Cr, Mo, W)

Xuefeng Wang and Lester Andrews*

Department of Chemistry, University of Virginia, Charlottesville, Virginia 22904-4319

Received: April 10, 2009; Revised Manuscript Received: June 2, 2009

Infrared absorptions of the matrix isolated SMO_2 (M = Cr, Mo, W) molecules were observed following laser-ablated metal atom reactions with SO_2 during condensation in solid argon and neon. The symmetric and antisymmetric M−O stretching mode assignments were confirmed by appropriate $S^{18}O_2$ and $S^{16,18}O_2$ isotopic shifts. The much weaker Cr−S stretching mode was identified through its ^{34}S shift. Density functional (B3LYP and BPW91) calculations were performed to obtain molecular structures and to reproduce the infrared spectra. Computed pyramidal structures for the SMO_2 molecules are very similar to those for the analogous trioxides and this functional group in $[MO_2S(bdt)]^{2-}$ complexes. Additional weaker absorptions are assigned to the $(SO_2)(SMO_2)$ adducts, which are stabilized by a four-membered ring.

Introduction

Tungsten and molybdenum enzymes have been investigated extensively because they play extremely important roles in life sciences. Oxo/sulfido ligands on tungsten and molybdenum centers are the oxidized sites in the xanthine oxidoreductase enzyme.[1,2] The complexes $[MO_2S(bdt)]^{2-}$ (M = Mo, W; bdt = benzene-1,2-dithiolate) have been successfully synthesized in a biomimetic approach to structural analogs of catalytic sites.[3] The terminal sulfido ligand is essential for enzymatic activity in the hydroxylation of C−H bonds in purines and related substrates and in the oxidation of aldehydes to acids.[4] However, accurate coordination structures at the W and Mo centers with proteins are not determined as near octahedral or near trigonal prismatic because the structure resolution is not sufficiently high.[5] It would be useful to have a simple model molecule for the $S_2WO_2^{2-}$ intermediate species in the synthesis of oxo/sulfido-dithiolene W^{VI} complexes, and we will present SWO_2 as such a simple molecule.

Because of the difference in d-orbital participation in σ-bonding and polarization of the outermost core shells, molybdenum and tungsten with hydrogen and methyl ligands favor trigonal prismatic structures (C_{3v}).[6−8] Reactions of Mo and W with NH_3, NF_3, and PF_3 gave major stable high oxidation state products, $N{\equiv}MH_3$, $N{\equiv}MF_3$ and $P{\equiv}MF_3$.[9] These structures violate the traditional VSEPR model. It is important to know the detailed structural features of active sites of tungsten and molybdenum enzymes in which the metal atom is coordinated by bioligand (dithiolene type) since the geometry of the molecule can influence their biological importance and activity. Kaupp has discussed the "non-VSEPR" distorted trigonal prismatic structure around the metal centers in molybdenum and tungsten enzymes.[5,10]

We present here a matrix infrared spectroscopic study of laser-ablated chromium, molybdenum, and tungsten atom reactions with SO_2 during condensation is excess argon and neon. The new metal sulfido oxides SMO_2 are identified from matrix isolation infrared spectroscopy with isotopic substitution and theoretical vibrational frequency calculations. The structure of SWO_2 calculated here is strikingly similar to that reported for this terminal functional group in the recently reported $[MO_2S(bdt)]^{2-}$ complexes.[3]

Experimental and Computational Methods

The experimental methods for investigating laser-ablated transition metal atom reactions with small molecules during condensation in excess argon or neon at 5 K have been described in our previous papers.[11,12] The Nd:YAG laser fundamental (1064 nm, 10 Hz repetition rate with 10 ns pulse width) was focused onto a rotating metal target (Johnson Matthey), which gave a bright plume spreading uniformly to the cold CsI window. The chromium, molybdenum, and tungsten targets were polished to remove oxide coating and immediately placed in the vacuum chamber. Sulfur dioxide (Matheson) was condensed and evacuated before dilution with research grade argon to make 0.4% samples or neon to give 0.2% mixtures. A mixture of $S^{18}O_2$ and $S^{16,18}O_2$ with a trace of $S^{16}O_2$ was prepared by tesla coil discharge of $^{18}O_2$ (YEDA) (about 1 Torr) in a 2 L pyrex bulb containing a film of sulfur sublimed onto the walls (about 5 mg) by external heating using a hot air gun. A sample of $^{34}SO_2$ was prepared from sulfur-34 (98% ^{34}S, Cambridge Isotope Laboratories) and oxygen. The laser energy was varied about 10−20 mJ/pulse. After sample deposition for one hour, FTIR spectra were recorded at 0.5 cm^{-1} resolution on a Nicolet 750 with 0.1 cm^{-1} accuracy using an MCT range B detector. Matrix samples were annealed at different temperatures and selected samples were subjected to photolysis by a medium pressure mercury arc lamp (Philips, 175 W) with globe removed.

Supporting density functional theory (DFT) calculations were performed using the Gaussian 03 program,[13] the B3LYP functional, the 6-311+G(3df) basis set for sulfur and oxygen atoms, and the SDD pseudopotential for chromium, molybdenum, and tungsten.[14−16] Complementary computations were done with the BPW91 density functional.[17] All of the geometrical parameters were fully optimized and the harmonic vibrational frequencies were obtained analytically at the optimized structures.

Results

Infrared spectra of laser-ablated chromium, molybdenum, and tungsten atom reaction products with SO_2 in excess argon or neon during condensation at 5 K will be presented in turn, and

---

* To whom correspondence should be addressed. E-mail: lsa@virginia.edu.

10.1021/jp9033408 CCC: $40.75

TABLE 1: Infrared Absorptions (cm^{-1}) Observed for Products of the Reaction of Cr, Mo, and W Atoms with SO_2 Molecules

SO_2/Ar	$S^{18}O_2$/Ar	$^{34}SO_2$/Ar	SO_2/Ne	assignment
		Cr		
1259.1	1212.6	1246.2	1270.6	$(SO_2)(SCrO_2)$
985.0	945.0	985.0	1003.6	$(SO_2)(SCrO_2)$
965.4	929.1	965.4	974.9	CrO_2
960.6	924.0	960.6	965.1	$SCrO_2$
957.9	921.2	957.9	971.8	$(SO_2)(SCrO_2)$
941.7	898.6	941.7	949.0	$SCrO_2^-$
937.7		937.7		
932.1	889.3	932.1	936.3	$SCrO_2$
895.4	854.6	895.4	902.5	$SCrO_2^-$
846.3	809.7	846.3		CrO
		Mo		
1254.0	1208.3	1242.4	1259.8	$(SO_2)(SMoO_2)$
975		975	981.1	$(SO_2)(SMoO_2)$
956		956	962.5	$(SO_2)(SMoO_2)$
940.3	892.8	940.3		$S^{92}MoO_2$
938.3	890.7	938.3		$S^{96}MoO_2$
937.3	889.7	937.3	945.0	$S^{98}MoO_2$
936.4	888.6	936.4	943.6	$S^{100}MoO_2$
913.5	872.4	913.5	919.0	$S^{92}MoO_2$
911.7	870.4	911.7	917.1	$S^{94}MoO_2$
910.7	869.5	910.7	916.4	$S^{95}MoO_2$
909.9	868.5	909.9	915.3	$S^{96}MoO_2$
908.9	867.6	908.9		$S^{97}MoO_2$
908.0	866.6	908.0	913.5	$S^{98}MoO_2$
906.2	864.8	906.2	911.7	$S^{100}MoO_2$
878.1	830.1	878.1	886	$SMoO_2^-$
		W		
1260.6	1216.4	1248.7	1265.6	$(SO_2)(SWO_2)$
993.8		993.8	999.2	$(SO_2)(SWO_2)$
972.4		972.4	972.9	$(SO_2)(SWO_2)$
964.6	913.0	964.6	973.1	SWO_2
921.6	875.3	921.6	927.6	SWO_2
903.6		903.6	904.5	SWO_2^-

the new product absorptions are listed in Table 1. Density functional calculations were performed to support the identification of new reaction products, and calculated frequencies are listed in Tables 2, 3, and 4. Common species in different experiments, such as SO, SOO, SO_3, and metal oxide bands have been identified in previous papers.[18-23] Experiments were also done with $S^{18}O_2$ and $^{34}SO_2$, and the isotopic frequencies are also listed in Table 1.

Cr + SO_2. Infrared spectra of laser-ablated chromium atoms codeposited with SO_2 in argon are shown in Figure 1. Two strong bands at 960.6 and 932.1 cm^{-1}, two medium strong bands at 941.7 and 895.4 cm^{-1}, and very weak bands at 985.0 and 957.9 cm^{-1} were observed in the Cr−O stretching region after deposition. These bands increased on annealing to 20 K by 50% and broadened on full-arc irradiation. Further annealing to 30 K increased dramatically the 960.6 and 932.1 cm^{-1} bands. Weak absorptions of CrO (846.3 cm^{-1}) and CrO_2 (965.3 and 914.4 cm^{-1}) were produced by the reaction since the $Cr^{18}O$ (809.7 cm^{-1}) and $Cr^{18}O_2$ (929.1 cm^{-1}) counterparts were also observed.[21]

Mo + SO_2. Figure 2 shows laser ablated Mo atom reactions with SO_2 in excess argon. New broad absorptions were observed centered at 938 and 908 cm^{-1} in the Mo═O stretching region on deposition. On annealing to 20 K, new bands appeared at 1254 and 975 cm^{-1}. These bands doubled on full-arc irradiation and further increased on annealing to 30 and 35 K. Figure 3 illustrates the resolved molybdenum isotopic splittings for the major product absorptions in the SO_2 and the mixed[16,18] SO_2 experiments. The Mo isotopic bands are given in Table 1. Similar experiments were done in a neon matrix, and the absorptions are listed in Table 1.

W + SO_2. As shown in Figure 4 and Table 1 the major reaction product absorptions of tungsten with SO_2 in solid argon are similar to that of chromium and molybdenum, but all of the observed bands are shifted to the blue because of stronger metal−oxygen double bonds in this group for tungsten. In solid neon, similar product absorptions were observed, Figure 5, with slight blue shifts. The sharp, photosensitive, 988.6 cm^{-1} band set is common to other metal experiments with SO_2 in solid neon and is near absorptions for the isolated SO_2^- anion.[20a]

Calculations. Density functional calculations were done for several possible products to assist in their identification. As shown in Figure 6, pyramidal C_s structures were obtained for the ($^1A'$) state SMO_2 molecules (M = Cr, Mo, W). The M−O and M−S bond lengths increase while SMO and OMO bond angles decrease from chromium to tungsten. These calculated structures are very similar to the group 6 MO_3 structures, which have been identified in our earlier papers.[22,23] This is the ground state for the Mo and W products, but a triplet state is 6 kcal/mol lower for Cr. Reaction energy profiles shown in Figure 7 include the M-SO_2 complexes and OM(SO) insertion products. Calculations were also done for (SO)(MO_2) complexes, which contain the SO subunit coordinated to MO_2 molecules, the (SO_2)(MO_2) complexes, and the (SO_2)(SMO_2) adducts, which are stabilized by a four-membered ring. Trends in calculated bond lengths and bond angles are the same as for the SMO_2 molecules. Finally the SMO_2^- molecular anions and the triatomic molecules SMO were calculated to assist in the search for new molecules.

Discussion

Infrared spectra of products formed in the reactions of laser-ablated Cr, Mo, and W atoms with SO_2 in excess argon and neon during condensation at 5 K will be assigned. Isotopic substitution and theoretical calculations were performed to support the identifications of new metal sulfide oxides.

SMO_2. The major product absorptions in these experiments are identified as SMO_2 molecules (M = Cr, Mo, and W) from isotopic spectra and comparison between calculated and observed frequencies using hybrid and pure density functionals as listed in Tables 1 and 2. The reactions are straightforward to give the final SMO_2 products with the metal centers in the VI oxidation state. The $SCrO_2$ molecule yield increases on annealing and on ultraviolet irradiation while the Mo and W counterparts increase on ultraviolet irradiation.

The mixed oxygen isotopic spectra clearly show that the new major products contain two equivalent oxygen atoms. This conclusion is reached from the asymmetric triplet isotopic M−O stretching absorptions shown at the top of Figures 1, 2, and 4. Both antisymmetric and symmetric M−O stretching absorptions are observed, and these couple for the mixed isotopic $SM^{16}O^{18}O$ molecules resulting in more separation and the asymmetric triplet structure.

Possible complexes of MO_2 molecules and the trace photoproduct SO or the reagent SO_2 must be ruled out before we can proceed. First, we form a very small amount of CrO_2 or $Cr^{16}O^{18}O$ and $Cr^{18}O_2$ in the chromium experiments, only 10% as much as the major product, based on calculated infrared intensities, and no detectable MoO_2 or WO_2. This makes a complex with trace SO extremely unlikely, and even with SO_2 still present in abundance, a complex with SO_2 and MO_2 is unlikely. Furthermore, the formation of SO_2−MO_2 complexes would require three reactions during formation of the matrix

TABLE 2: Calculated Frequencies of the SMO_2 ($^1A'$) Molecules (M = Cr, Mo, W) in C_s Symmetry[a]

B3LYP			BPW91		
16-O	18-O	16-O, 34-S	16-O	18-O	mode assignment
$SCrO_2$					
1057.2(210)	1016.6(195)	1057.2(210)	1015.6(168)	976.2(155)	Cr=O str, a''
1038.1(155)	989.5(144)	1038.1(155)	990.6(124)	944.5(116)	Cr=O str, a'
580.9(25)	578.0(24)	571.8(24)	567.7(25)	565.2(24)	Cr=S str, a'
375.3(5)	341.2(4)	355.7(5)	349.5(4)	333.5(3)	CrO_2 bend, a'
265.2(1)	256.3(1)	263.2(1)	263.4(1)	254.4(1)	SCrO def, a''
192.2(33)	187.2(31)	191.6(33)	221.3(23)	215.4(22)	$SCrO_2$ def, a''
$S^{98}MoO_2$					
980.3(139)	930.1(127)	980.3(139)	947.3(111)	899.0(102)	Mo=O str, a'
950.8(188)	906.8(172)	950.8(188)	923.4(152)	880.5(139)	Mo=O str, a''
539.8(40)	539.1(40)	528.5(39)	528.6(34)	528.0(34)	Mo=S str, a'
322.6(3)	306.6(2)	312.9(3)	318.9(2)	303.0(2)	MoO_2 bend, a'
246.8(0)	238.2(0)	244.8(0)	244.2(0)	235.7(0)	SMoO def, a''
216.7(17)	209.5(16)	215.7(17)	227.4(12)	220.0(11)	$SMoO_2$ def, a''
SWO_2					
984.5(102)	931.7(91)	984.5(102)	951.4(81)	900.3(73)	W=O str, a'
939.4(148)	891.4(134)	939.4(148)	912.3(120)	865.6(108)	W=O str, a''
512.4(32)	512.1(32)	499.9(31)	503.8(26)	503.6(26)	W=S str, a'
328.5(3)	311.3(2)	328.1(3)	325.4(2)	308.3(2)	WO_2 bend, a'
246.8(0)	237.8(0)	244.7(0)	245.3(0)	236.4(0)	SWO def, a''
230.3(12)	221.7(10)	229.2(12)	237.2(8)	228.3(7)	SWO_2 def, a''

[a] Frequencies in cm^{-1} with (intensities, km/mol). B3LYP functional, the 6-311+G(3df) basis set for sulfur and oxygen atoms, and the SDD pseudopotential for chromium, molybdenum, and tungsten were used.

TABLE 3: Calculated Frequencies for the SMO_2^- ($^1A_1$) Anions (M = Cr, Mo, W) in C_{2v} Symmetry[a]

B3LYP			BPW91		
16-O	18-O	16-O, 34-S	16-O	18-O	mode assignment
$SCrO_2^-$					
992(308)	954(281)	992(309)	972(252)	935(230)	Cr=O str, b_2
958(225)	913(207)	957(225)	928(185)	885(173)	Cr=O str, a_1
492(19)	488(18)	485(218)	514(32)	509(30)	Cr=S str, a_1
320(4)	307(4)	318(4)	309(4)	296(4)	CrO_2 bend, a_1
223(0)	215(0)	221(0)	215(0)	207(0)	SCrO def, b_2
128(34)	125(31)	128(34)	85(23)	83(21)	$SCrO_2$ def, b_1
$S^{98}MoO_2^-$					
917(205)	869(187)	917(205)	886(174)	840(159)	Mo=O str, a_1
906(293)	865(265)	906(293)	882(250)	842(226)	Mo=O str, b_2
499(66)	497(65)	489(62)	489(55)	487(54)	Mo=S str, a_1
SWO_2^-					
926(177)	876(159)	926(177)	895(154)	847(214)	W=O str, a_1
892(264)	848(237)	892(264)	867(230)	824(206)	W=O str, b_2
480(77)	479(76)	469(72)	470(64)	469(63)	W=S str, a_1

[a] Frequencies in cm^{-1} with (intensities, km/mol). B3LYP functional, the 6-311+G(3df) basis set for sulfur and oxygen atoms, and the SDD pseudopotential for chromium, molybdenum, and tungsten were used.

TABLE 4: Calculated Frequencies for the SMO ($^3A''$) Molecules (M = Cr, Mo, W)[a]

B3LYP			BPW91		
16-O	18-O	16-O, 34-S	16-O	18-O	mode assignment
SCrO					
986.7(287)	944.5(267)	986.6(287)	984.7(194)	942.6(181)	Cr=O str
530.5(11)	529.5(10)	521.0(11)	543.6(23)	542.8(22)	Cr=S str
193.8(3)	187.8(2)	192.5(3)	223.7(1)	216.6(1)	S−M−O bend
$S^{98}MoO$					
971.0(199)	923.4(181)	971.0(199)	945.6(153)	899.3(140)	Mo=O str
539.0(59)	538.8(58)	527.3(56)	531.7(43)	531.5(42)	Mo=S str
235.8(1)	227.4(0)	234.2(1)	240.9(1)	232.3(1)	S−M−O bend
SWO					
977.5(149)	926.1(134)	977.4(149)	949.4(118)	899.5(106)	W=O str
525.6(44)	525.5(44)	512.5(42)	517.2(33)	517.1(33)	W=S str
240.3(3)	231.0(2)	238.8(3)	239.7(2)	230.4(2)	S−M−O bend

[a] B3LYP functional, the 6-311+G(3df) basis set for sulfur and oxygen atoms, and the SDD pseudopotential for chromium, molybdenum, and tungsten were used.

sample, M with SO_2 to form MO and SO, MO with SO_2 to give MO_2, and then MO_2 with SO_2 to form the final complex, whereas the concerted reaction proposed here requires a single step. Frequency calculations for the SO_2-CrO_2 complex predict the intense modes 20−30 cm^{-1} higher still than for $SCrO_2$ and make this complex an even longer shot. Finally, the observation of a terminal Cr−S stretching mode for the $CrSO_2$ molecule is conclusive and rules out assignment to $SO-CrO_2$ or SO_2-CrO_2 complexes where such a mode does not exist.

The antisymmetric and symmetric stretching vibrations of the CrO_2 subunit of $SCrO_2$ were observed at 960.6 and 932.1 cm^{-1}, respectively, in solid argon, which are 4.8 lower and 17.7 cm^{-1} higher and thus separated less than the stretching frequencies of molecular CrO_2 isolated in solid argon.[21] This suggests that the O−Cr−O bond angle in $SCrO_2$ is less than the same bond angle in the CrO_2 molecule. An experiment using $^{34}SO_2$ gave the same strong bands without shifts. Our DFT/B3LYP calculation predicts the O−Cr−O bond angle in singlet $SCrO_2$ as 113.9°, which is much smaller than 132° for triplet CrO_2 estimated by B3LYP calculations.[23] A similar computation predicts the O−Cr−O angle in singlet CrO_3 as 114.2°. With ^{18}O-enriched sample, these two bands shifted to 924.0 and 889.3 cm^{-1} giving 1.0396 and 1.0481 $^{16}O/^{18}O$ isotopic ratios, which are near the 1.0399 and 1.0491 ratios from computed frequencies. As shown in Figure 1, where there is about 5% SO_2 and 20% $S^{16,18}O_2$ in the sample, triplet oxygen isotopic distributions were observed for the two bands, which indicates the participation of two equivalent oxygen atoms. The mixed oxygen isotopic bands at 951.8 and 901.2 cm^{-1} are displaced away from the median position owing to their interaction in the mixed isotopic molecule, and our calculation predicts these modes to be separated by 49.9 cm^{-1}. The observed 960.6/951.8 = 1.0092 and 932.1/901.2 = 1.0343 ratios are very near the 1.0067 and 1.0377 ratios of calculated frequencies for the normal and mixed oxygen isotopic molecules. Thus, the stronger and weaker bands

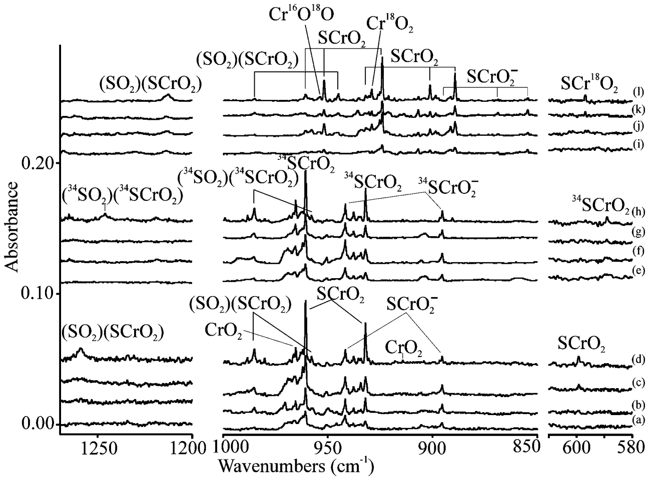

Figure 1. Infrared spectra for the chromium atom and SO_2 reaction products in solid argon at 5 K. (a) Cr + SO_2 deposition for 60 min; (b) after annealing to 20 K; (c) after >220 nm irradiation; (d) after annealing to 35 K; (e) Cr + $^{34}SO_2$ deposition for 60 min; (f) after annealing to 20 K; (g) after >220 nm irradiation; (h) after annealing to 35 K; (i) Cr + $S^{16,18}O_2$ deposition for 60 min; (j) after annealing to 20 K; (k) after >220 nm irradiation; (l) after annealing to 35 K.

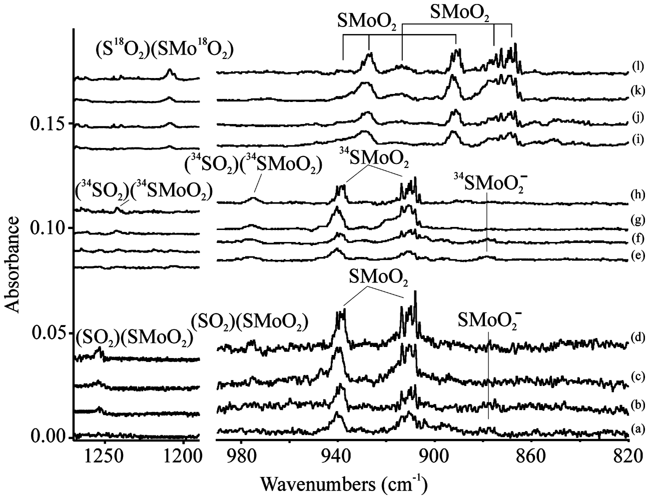

Figure 2. Infrared spectra for the molybdenum atom and SO_2 reaction products in solid argon at 5 K. (a) Mo + SO_2 deposition for 60 min; (b) after annealing to 20 K; (c) after >220 nm irradiation; (d) after annealing to 35 K; (e) Mo + $^{34}SO_2$ deposition for 60 min; (f) after annealing to 20 K; (g) after >220 nm irradiation; (h) after annealing to 35 K; (i) Mo + $S^{16,18}O_2$ deposition for 60 min; (j) after annealing to 20 K; (k) after >220 nm irradiation; (l) after annealing to 35 K.

at 960.6 and 932.1 cm^{-1}, respectively, in solid argon are assigned to the antisymmetric and symmetric Cr−O stretching modes of the $SCrO_2$ molecule.

Very weak bands were observed at 599.2, 596.9, and 589.1 cm^{-1} in the experiments with SO_2, $S^{18}O_2$, and $^{34}SO_2$, and these bands tracked on annealing with the stronger Cr−O stretching modes assigned above (Figure 1). The Cr−S stretching mode is predicted to be an order of magnitude weaker at 580.9, 578.0, and 571.8 cm^{-1} for the above isotopic modifications in the singlet state, and this agreement is acceptable. On the basis of isotopic shifts, the Cr−S stretching mode is slightly coupled to oxygen motion, but the higher frequency Cr−O stretching modes are not coupled to sulfur. The present 599 cm^{-1} band may be compared with the 575 cm^{-1} antisymmetric fundamental observed for CrS_2 and the B3LYP prediction 32 cm^{-1} lower than the observed value.[25]

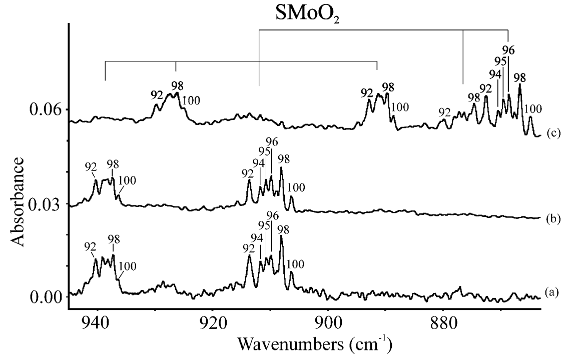

Figure 3. Infrared spectra for natural Mo atom reaction product with SO_2 in the 945−863 cm^{-1} regions using expanded wavenumber scale. (a) Spectrum from Figure 2d, (b) spectrum from Figure 2h, and (c) spectrum from Figure 2l.

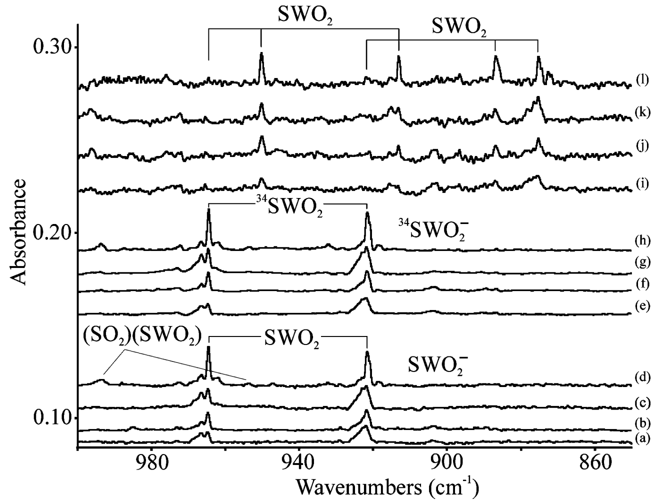

Figure 4. Infrared spectra for the tungsten atom and SO_2 reaction products in solid argon at 5 K. (a) W + SO_2 deposition for 60 min; (b) after annealing to 20 K; (c) after >220 nm irradiation; (d) after annealing to 35 K; (e) W + $^{34}SO_2$ deposition for 60 min; (f) after annealing to 20 K; (g) after >220 nm irradiation; (h) after annealing to 35 K; (i) W + $S^{16,18}O_2$ deposition for 60 min; (j) after annealing to 20 K; (k) after >220 nm irradiation; (l) after annealing to 35 K.

In the neon matrix, the two Cr−O stretching modes of the $SCrO_2$ molecule are observed at 965.1 and 936.3 cm^{-1}, which are similar to the argon−neon matrix shifts observed for group 6 metal oxides and other small molecules.[23,24] These values are slightly lower than the 991.3 cm^{-1} observation of the antisymmetric stretching mode for CrO_3 in solid neon.[23]

Our DFT calculation at B3LYP/SDD/6-311+G(3df) level of theory predicted Cr−O stretching modes for $SCrO_2$ at 1057.0 and 1042.3 cm^{-1}, respectively, which are overestimated by 9.5 and 10.2%. In like manner, our calculation for CrO_3 predicted the antisymmetric fundamental 8.2% higher and for CrO_2 4.8% higher than the neon matrix observations.[24] With the all electron 6-311+G(3df) basis at the B3LYP level, the calculation gave almost the same values for the two Cr=O stretching modes at 1057.2 and 1038.1 cm^{-1}. The BPW91 functional (Table 2) produced lower frequencies in better agreement (5.7 and 6.3% high) with the observed values, as expected.[26]

Our B3LYP calculation finds a $^3A''$ state 6 kcal/mol lower in energy, but the two Cr−O stretching modes computed at 1049 cm^{-1} (254 km/mol) and 1044 cm^{-1} (70 km/mol) do not show the correct mode separation and relative intensity and the Cr−S stretching mode is predicted 128 cm^{-1} lower than observed. In addition, our BPW91 calculation locates this triplet state 8 kcal/

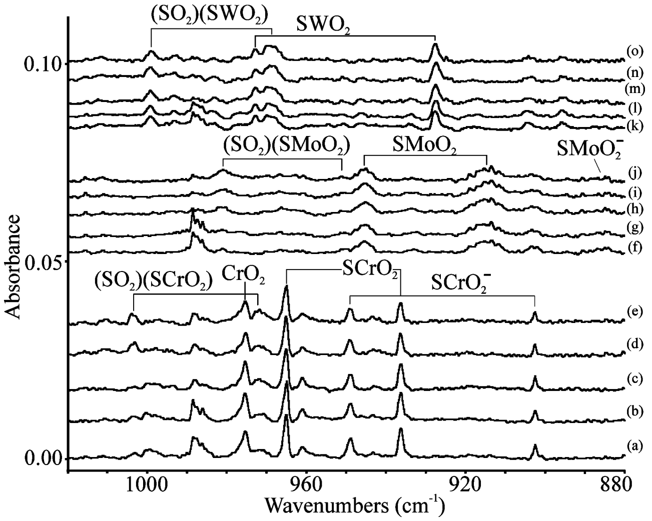

Figure 5. Infrared spectra for the group 6 atom and SO$_2$ reaction products in solid neon at 5 K. (a) Cr + SO$_2$ deposition for 60 min; (b) after annealing to 8 K; (c) after >470 nm irradiation; (d) after >240−380 nm irradiation; (e) after annealing to 10 K; (f) Mo + SO$_2$ deposition for 60 min; (g) after annealing to 8 K; (h) after >320 nm irradiation; (i) after >240−380 nm irradiation; (j) after annealing to 10 K; (k) W + SO$_2$ deposition for 60 min; (l) after annealing to 8 K; (m) after >320 nm irradiation; (n) after >240−380 nm irradiation; (o) after annealing to 10 K.

mol higher than the singlet state with 984 cm^{-1} (170 km/mol) and 979 cm^{-1} (28 km/mol) frequencies. The relative intensities and Cr−O mode separations and Cr−S mode for both calculations for the singlet state (Table 2) fit the observed absorptions much better, and the singlet SCrO$_2$ ground state is identified accordingly, which is in agreement with the Mo and W counterparts below.

In solid argon, the reaction of Mo atom with SO$_2$ gave a set of bands at 906.2, 908.0, 908.9, 909.9, 910.7, 911.7, and 913.5 cm^{-1}, which increased on annealing and the relative intensities of the seven-peak pattern in Figure 3 correspond with the statistical distribution of natural Mo isotopes in natural abundance.[9b] These resolved absorptions indicate that a single Mo atom participates in the vibrational mode and show that the product molecule is cleanly isolated in the matrix. A set of higher bands at 936.4, 937.3, 938.3, and 940.3 cm^{-1} tracked with the above set of bands but a smaller Mo isotopic splitting was observed. These Mo isotopic splittings agree (to 0.1 cm^{-1}) with those reported for the strong antisymmetric (894.0 cm^{-1}) and symmetric (939.3 cm^{-1}) stretching bands for ^{98}MoO$_2$ in solid argon.[22] With ^{18}O enriched sample (5% SO$_2$, 20% S^{16,18}O$_2$, and 75% S^{18}O$_2$), all of these bands show shifts, and the ^{16}O/^{18}O isotopic ratios for the main bands are 1.0478 and 1.0535, which may be compared to the calculated ratios of 1.0485 and 1.0540, respectively. The mixed isotopic SMo^{16}O^{18}O bands were also observed, separated from the median positions as before, with S^{98}Mo^{16}O^{18}O counterparts at 874.5 and 926.2 cm^{-1} and the same Mo isotopic intervals, and the triplet oxygen isotopic pattern demonstrates two equivalent oxygen atoms and suggests the SMoO$_2$ assignments. In solid neon, the two Mo−O stretching modes (due to S^{98}MoO$_2$) are blue shifted to 913.5 and 945.0 cm^{-1}. Finally, the Mo−S stretching mode is too weak to be observed on the blue wing of the strong sulfur dioxide band at 517 cm^{-1}.

Our B3LYP calculation predicted two Mo−O stretching modes at 950.8 and 980.3 cm^{-1}, which are only overestimated by 4.1 and 3.7%, respectively, and the BPW91 functional found these modes lower at 923.4 and 947.3 cm^{-1}, which are 1.7 and 1.1% higher than the observed values. For MoO$_3$, our B3LYP antisymmetric mode is 6.1% above the neon matrix value. Such favorable agreement is often observed for new molecules containing transition metal atoms.[25−28]

The absorptions due to SWO$_2$ were found at 921.6 and 964.6 cm^{-1} in solid argon, which are 56.3 and 60.4 cm^{-1} lower than the same modes observed for WO$_2$ molecules.[24] In solid neon, these two modes were observed at 927.6 and 973.1 cm^{-1}, respectively, which are 56.3 and 57.2 cm^{-1} below the analogous stretching modes for WO$_2$ in solid neon. With S^{18}O$_2$ in solid argon the two modes shift to 875.3 and 913.0 cm^{-1}, giving 1.0529 and 1.0565 ^{16}O/^{18}O ratios. The mixed isotopic bands at 886.7 and 950.2 cm^{-1} complete triplet oxygen isotopic distributions for both modes and verify the SWO$_2$ assignment. Our B3LYP calculation predicted two W−O stretching modes at 939.4 and 984.5 cm^{-1}, overestimated by only 1.3 and 1.2%, but the BPW91 calculation found these modes about 10 cm^{-1} lower than the observed bands. Our B3LYP calculation for WO$_3$ predicted the antisymmetric mode 0.9% above the neon matrix value. Such vibrational frequency calculations are only an approximation, but they are a very good approximation and support our assignments. Note that the W−O stretching modes in SWO$_2$ were observed to be lower than the same modes for WO$_2$, which are in contrast to the molybdenum case.

The calculation of vibrational frequencies is not an exact science, and group 6 metal containing molecules present a particular challenge.[27−31] The correlation of B3LYP and BPW91 hybrid and pure density functional computed and observed frequencies for the major SMO$_2$ product molecules given above is comparable to that found for the binary CrO$_2$, CrO$_3$, MoO$_3$, and WO$_3$ molecules,[23] and this level of agreement between calculated and observed matrix frequencies is all that we can expect of the density functional approximation where we have a lot of experience.[27−31] Accounting for anharmonicity in the calculation and matrix shifts in the observed frequencies should improve the agreement between the two methods. There is a range of opinion on this subject as one referee found the agreement "supportive but far from compelling" and the other "DFT calculations have sufficient reliability and predictability to make the experiments unnecessary." Clearly we need to continue to compare observed and calculated frequencies and to revalidate the identification and prediction of new molecules using both scientific methods.

The insertion reactions of M (M = Cr, Mo, W) atoms into SO$_2$ to give SMO$_2$ are exothermic by 18 kcal/mol (Cr), 109 kcal/mol (Mo), and 159 kcal/mol (W), respectively, based on B3LYP calculations. The reactions likely proceed on first insertion to give OMSO, and then rearrange to produce the final stable SMO$_2$ molecules

$$\mathrm{M} + \mathrm{SO_2} \rightarrow \mathrm{OMSO} \rightarrow \mathrm{SMO_2} \qquad (1)$$

SMO$_2^-$. The next strongest absorptions on deposition of Cr + SO$_2$ in solid argon at 941.7 and 895.4 cm^{-1} showed little change on UV irradiation in contrast to the SCrO$_2$ bands and decreased on further annealing to 30 K while the SCrO$_2$ bands increased substantially. These bands increased relative to the SCrO$_2$ bands with higher laser energy. In solid neon, analogous bands appeared with comparable intensities, slightly blue shifted to 949.0 and 902.5 cm^{-1}. The former absorptions did not shift with sulfur-34 but shifted to 906.8 and 854.6 cm^{-1} on full-O-18 substitution, defining 1.0385 and 1.0479 ratios for antisymmetric and symmetric Cr−O stretching modes. One mixed O-16,

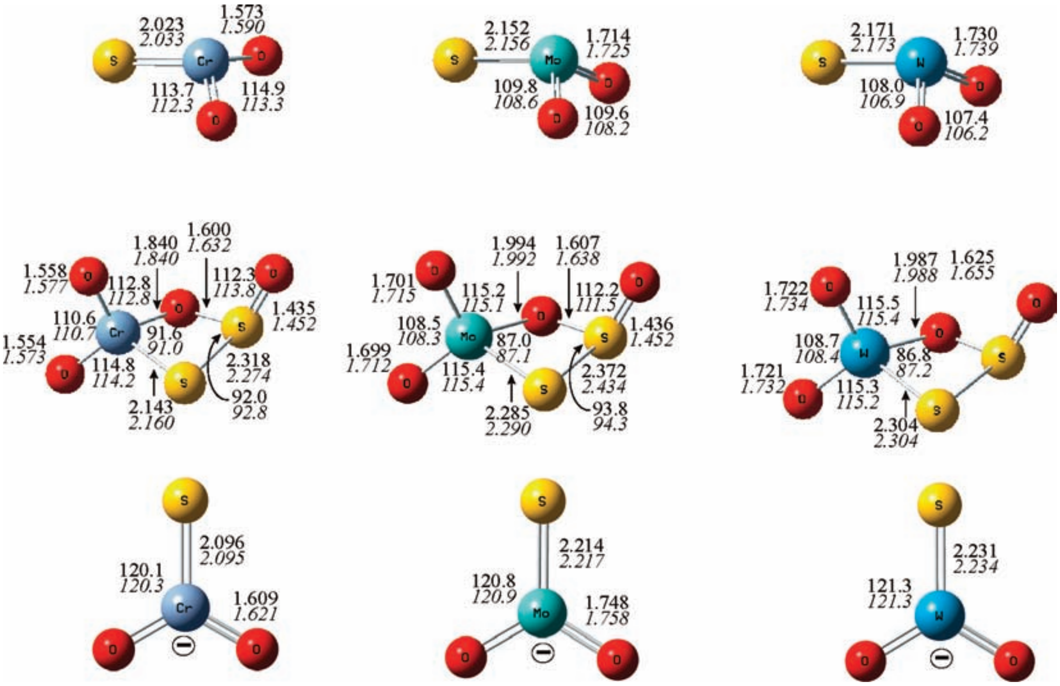

Figure 6. Structures calculated using B3LYP and BPW91 (italic values) methods.

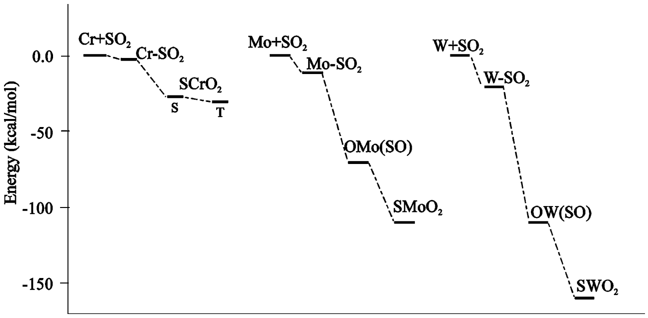

Figure 7. Energy profile of group 6 metal atom and SO_2 reaction products computed at the B3LYP level of theory relative to the energy of the metal atom and the reagent molecule.

18 band was observed at 868.7 cm^{-1}, which is below the median position and gives a 895.5/868.7 = 1.0309 ratio. These bands are appropriate for the two Cr−O stretching vibrations of a new $XCrO_2$ molecule, which has lower frequencies than $SCrO_2$ itself. Since many complexes with CrO_2 are blue shifted and the CrO_2^- anion is stable to UV irradiation,[21,23] we performed calculations for the $SCrO_2^-$ molecular anion. The red-shifted modes computed for $SCrO_2^-$ follow the pattern for CrO_2^- relative to CrO_3 itself.[23] Our B3LYP calculation predicts the two stretching modes for $SCrO_2^-$ 5.3 and 6.9% high and the BPW91 calculation finds these modes 3.2 and 3.7% high, which is better agreement than found for $SCrO_2$ itself. The computed ratio for the all-16/16, 18 mode at 1.0389 is just above the observed ratio, which provides a measure of coupling between the two vibrational modes.

A weak broadband centered at 878.1 cm^{-1} appeared on deposition of laser-ablated Mo reaction with SO_2 in solid argon. The broad feature must contain the Mo isotopic involvement, but we cannot identify these details because of band weakness. A similar B3LYP calculation for $SMoO_2^-$ predicts this antisymmetric Mo−O stretching mode at 906 cm^{-1}, which is acceptable agreement.

A sharper band at 903.6 cm^{-1} appeared on deposition of laser-ablated W in solid argon, decreased on annealing to 20 K, and disappeared on full-arc irradiation. This mode is predicted at 893 cm^{-1} for SWO_2^- by B3LYP.

In the laser-ablation process, electrons are produced and anions are often trapped.[12] The isolated SO_2^- anion is identified in all of our neon matrix experiments at 988.6 cm^{-1},[20a] and the metal atom reaction with this anion follows. These are stable anions with computed electron affinities of 96, 82, and 85 kcal/mol, respectively for the SMO_2 molecules, which are comparable to the electron affinity for CrO_3.[23] The SMO_2^- anion is probably made in our experiments by reaction 2

$$M + SO_2^- \rightarrow SMO_2^- \qquad (2)$$

$(SO_2)SMO_2$. In laser-ablated Cr atom reactions with SO_2 in solid argon, three absorptions at 1259.1, 985.0, and 957.9 cm^{-1} appeared very weakly on deposition, increased 5× on annealing to 20 K, slightly on full-arc irradiation, and increased another 4× together on annealing to 30 K. The 1259.1 cm^{-1} band is appropriate for an S−O stretching vibration and the 985.0 and 957.9 cm^{-1} bands are due to Cr−O stretching vibrations based on isotopic shifts. With $^{34}SO_2$ sample, the 1259.1 cm^{-1} band shifts to 1249.2 cm^{-1} while no shifts are found for the other two bands. With $S^{18}O_2$ sample, the three bands shift to 1208.3, 945.1, and 921.2 cm^{-1}, respectively. The isotopic distribution for the strongest 985.0 cm^{-1} band with mixed 16-18 sample shows a doublet at 984.9 and 945.1 cm^{-1}. These bands are assigned to the $(SO_2)SCrO_2$ molecule. DFT calculations support this assignment. The B3LYP calculation predicted Cr−O stretching modes at 1092.9 and 1079.2 cm^{-1} and a terminal S−O stretching mode at 1284.1 cm^{-1}, which match the observed values reasonably well.

Two broad bands centered at 975 and 956 cm^{-1} (isotopic Mo−O stretching vibrations) track with the 1254 cm^{-1} band (S−O stretching vibration). These bands appeared on annealing at 30 and 35 K and are assigned to Mo−O stretching and S−O stretching modes of the $(SO_2)SMoO_2$ molecule. With $^{34}SO_2$ sample, the 1254 cm^{-1} band (S−O mode) shifted to 1242.4 cm^{-1} while the 975 and 956 cm^{-1} bands (Mo−O modes) showed no shift. With $S^{18}O_2$ sample, the 1254 cm^{-1} band appeared at 1208.3 cm^{-1}, but absorptions for Mo−O stretching modes are overlapped by broad bands of isotopic $SMoO_2$ molecules. In solid neon, three bands at 1259.8, 981.1, and 962.5 cm^{-1} are appropriate for $(SO_2)SMoO_2$ molecule. DFT calculation was performed for $MoO_2(SO)_2$ (Figure 6), and two strong Mo−O stretching modes were calculated at 1009.3 and 991.7 cm^{-1} and one S−O stretching mode at 1281.3 cm^{-1}, which are very close to our observed values.

Weak absorptions due to $(SO_2)SWO_2$ were found at 1260.6 (S−O stretching), 993.8, and 972.4 (W−O stretching) cm^{-1}. The S−O stretching frequency at 1260.6 cm^{-1} shifts to 1216.4 cm^{-1} with $S^{18}O_2$ sample and 1248.7 cm^{-1} with $^{34}SO_2$ sample. However the W−O stretching modes are too weak to measure in the $S^{18}O_2$ experiment. In solid neon, new absorptions at 1265.6, 999.2, and 972.9 cm^{-1} were observed for the $(SO_2)SWO_2$ molecule. The assignment of $(SO_2)SWO_2$ is nicely supported by DFT calculations. The three strongest IR active modes are at 1283.3 cm^{-1} (S−O stretching), 1006.3 and 977.2 cm^{-1} (W−O stretching), which match the observed values very well.

The $(SO_2)SMO_2$ molecules can in principle be formed by adding SO_2 to SMO_2. No significant activation energy is required since spontaneous formation of this product is observed on annealing for all three metals. Our B3LYP calculations predict the reactions to be exothermic by 37 kcal/mol (Cr), 42 kcal/mol(Mo), and 47 kcal/mol (W).

$$SMO_2 + SO_2 \rightarrow (SO_2)SMO_2 \qquad (3)$$

Bonding. Cr, Mo, and W atoms react with SO_2 to give the common product SMO_2, suggesting the same reaction mechanism. As we know the third row 3d orbital is corelike and less reactive while fourth row 4d and fifth row 5d orbitals are involved in bonding in most reactions. However the group 6 metal atom reactions with SO_2 are driven by the high electronegativity of O and S atoms, and as a result, the outermost d orbitals are activated. The exothermic reaction energy increases in the series Cr−Mo−W, only 18 kcal/mol for Cr but 109 kcal/mol for Mo and 159 kcal/mol for W, suggesting considerable bond energy increases, which are consistent with group 6 metal atom and NF_3 reaction energies.[9b]

This contrasts sharply group 6 metal atom reactions with H_2, which gave valence-bonded WH_6 and MoH_6 trigonal prismatic C_{3v} structures with low electron spin states and only the hydride complex $CrH_2(H_2)_2$ with high electron spin state.[6] This evidence shows that d electrons for W and Mo form orthogonal sd^5 hybrids while 3d orbitals for Cr are not strongly involved in bonding. A similar trend is obtained from reactions with H_2O_2 where W + H_2O_2 gives H_2WO_2 while the hydroxide $Cr(OH)_2$ is the most stable form as the 3d orbital is corelike and less reactive.[30]

Note that all three SMO_2 molecules are stabilized as nonplanar (prismatic) structures with C_s symmetry. Clearly the structure of SMO_2 is derived from the prismatic structural preference (nonoctahedral) observed for WH_6 and MoH_6. The O−M−O and S−M−O bond angles are decreased in the series Cr−Mo−W, which reflects the d orbital participation in bonding and polarization of the outermost core shell. As expected, the 5d orbital is the most expanded of all three metal atoms, therefore the W═O and W═S bonds are more ionic, while Cr═O and Cr═S bonds are more covalent. The NBO analysis of bond type and bond orbitals for SMO_2 molecules and Mulliken charges are listed in Table 5. On the basis of calculation, the d orbital participation in bonding increases from Cr to Mo and then decreases to W while polarization of the outermost core shell increases straightforwardly from Cr to W. Thereby the prismatic structure is expected.

TABLE 5: Calculated (B3LYP) Bond Type, Bond Orbitals and Mulliken Charges for $SCrO_2$, $SMoO_2$, and SWO_2[a]

bond	bond type	bond orbital	Mulliken charges
		$SCrO_2$	
Cr═O	σ bond	(31.5%)Cr, s(20%)d(80%)	Cr: 1.598
		(68.5%)O, s(13%)p(86%)	O: −0.574
	π bond	(32.8%)Cr, s(4%)d(95%)	S: −0.451
		(67.2%)O, s(0%)p(100%)	
Cr═S	σ bond	(36.9%)Cr, s(48%)d(51%)	
		(63.1%)S, s(8%)p(91%)	
	π bond	(43.7%)Cr, s(0%)d(99%)	
		(56.3%)S, s(3%)p(97%)	
		$SMoO_2$	
Mo═O	σ bond	(26.8%)Mo, s(15%)d(85%)	Mo: 2.173
		(73.2%)O, s(17%)p(83%)	O: −0.729
	π bond	(30.1%)Mo, s(10%)d(90%)	S: −0.715
		(69.9%)O, s(1%)p(99%)	
Mo═S	σ bond	(33.4%)Mo, s(47%)d(52%)	
		(66.6%)S, s(12%)p(87%)	
	π bond	(39.2%)Mo, s(1%)d(98%)	
		(60.8%)O, s(1%)p(99%)	
		SWO_2	
W═O	σ bond	(24.5%)W, s(21%)d(79%)	W: 2.443
		(75.5%)O, s(21%)p(79%)	O: −0.857
	π bond	(29.8%)W, s(5%)d(95%)	S: −0.729
		(70.2%)O, s(0%)p(100%)	
W═S	σ bond	(36.0%)W, s(47%)d(52%)	
		(64.0%)S, s(12%)p(87%)	
	π bond	(35.3%)W, s(0%)d(99%)	
		(64.7%)S, s(2%)p(97%)	

[a] A similar analysis using the BPW91 functional gave orbital percentages within 1%.

Conclusions

Laser-ablated group 6 metal atoms react with SO_2 during condensation in excess argon and neon to form the SMO_2 (M = Cr, Mo, W) molecules as the major product. Strong absorptions in the matrix infrared spectra are assigned to symmetric and antisymmetric M-O stretching modes through appropriate $S^{18}O_2$ and $S^{16,18}O_2$ isotopic shifts. The much weaker Cr−S stretching mode in the $SCrO_2$ molecule was identified from its ^{34}S shift. This significant observation rules out assignment to a metal dioxide complex. Density functional (B3LYP and BPW91) calculations obtained C_s molecular structures and frequencies to support assignment of the infrared spectra. Although the calculation of vibrational frequencies is not an exact science, particularly for group 6 metal containing molecules, the correlation of frequencies from hybrid and pure density functionals with observed spectra substantiates the identification of these new molecules. Computed pyramidal structures for the SMO_2 molecules are very similar to those for the analogous trioxides and this functional group structure in the recently reported $[MO_2S(bdt)]^{2-}$ complexes.[3] Additional weaker absorptions are assigned to the $(SO_2)(SMO_2)$ adducts, which are stabilized by a four-membered ring, and the SMO_2^- molecular anions.

Acknowledgment. We gratefully acknowledge financial support from Subgrant No. 6855694 under Prime Contract No. DE-AC02-05CH11231 to the Lawrence Berkeley National

Laboratory from the DOE and NCSA computing Grant CHE07-0004N to L.A.

References and Notes

(1) Hille, R. *Chem. Rev.* **1996**, *96*, 2757, and references therein (Mo enzymes).

(2) Johnson, M. K.; Rees, D. C.; Adams, W. W. *Chem. Rev.* **1996**, *96*, 2817, and references therein (W enzymes).

(3) Groysman, S.; Wang, J. J.; Tagore, R.; Lee, S. C.; Holm, R. H. *J. Am. Chem. Soc.* **2008**, *130*, 12794.

(4) Hille, R. *Eur. J. Inorg. Chem.* **2006**, 1913.

(5) Kaupp, M. *Angew. Chem., Int. Ed.* **2001**, *40*, 3534.

(6) (a) Wang, X.; Andrews, L. *J. Am. Chem. Soc.* **2002**, *124*, 5636. (b) Wang, X.; Andrews, L. *J. Phys. Chem. A* **2002**, *106*, 6720 (WH_2, WH_4, and WH_6 in solid argon and neon). (c) Wang, X.; Andrews, L. *J. Phys. Chem. A* **2003**, *107*, 570 (Cr + H_2). (d) Wang, X.; Andrews, L. *J. Phys. Chem. A* **2005**, *109*, 9021 (Mo + H_2).

(7) (a) Shen, M.; Schaefer, H. F., III.; Partridge, H. *J. Chem. Phys.* **1993**, *98*, 508. (b) Kang, S. K.; Tang, H.; Albright, T. A. *J. Am. Chem. Soc.* **1993**, *115*, 1971. (c) Tanpipat, N.; Baker, J. *J. Phys. Chem.* **1996**, *100*, 19818. (d) Kaupp, M. *J. Am. Chem. Soc.* **1996**, *118*, 3018 WH_6 theoretical calculations.

(8) (a) Cho, H. G.; Andrews, L. *Inorg. Chem.* **2005**, *44*, 7634 (Cr, W + CH_4). (b) Cho, H. G.; Andrews, L. *J. Am. Chem. Soc.* **2005**, *127*, 8726 (Mo + CH_4).

(9) (a) Wang, X.; Andrews, L. *Organometallics* **2008**, *27*, 4885 (Cr, Mo, W + NH_3). (b) Wang, X.; Andrews, L.; Lindh, R.; Veryazov, V.; Roos, B. O. *J. Phys. Chem A* **2008**, *112*, 8030 (Cr, Mo, W + NF_3, PF_3).

(10) Straka, M.; Hrobarik, P.; Kaupp, M. *J. Am. Chem. Soc.* **2005**, *127*, 2591.

(11) Andrews, L. *Chem. Soc. Rev.* **2004**, *33*, 123.

(12) Andrews, L.; Citra, A. *Chem. Rev.* **2002**, *102*, 885.

(13) Frisch, M. J. et al. *Gaussian 03*, rev. D.01, Gaussian, Inc.: Pittsburgh, PA, 2004.

(14) (a) Becke, A. D. *J. Chem. Phys.* **1993**, *98*, 5648. (b) Lee, C.; Yang, Y.; Parr, R. G. *Phys. Rev. B* **1988**, *37*, 785.

(15) Frisch, M. J.; Pople, J. A.; Binkley, J. S. *J. Chem. Phys.* **1984**, *80*, 3265.

(16) Andrae, D.; Haeussermann, U.; Dolg, M.; Stoll, H.; Preuss, H. *Theor. Chim. Acta* **1990**, *77*, 123.

(17) (a) Becke, A. D. *Phys. Rev. A* **1988**, *38*, 3098. (b) Perdew, J. P.; Burke, K.; Wang, Y. *Phys. Rev. B* **1996**, *54*, 16533, and references therein. (c) see also Becke, A. D. *J. Chem. Phys.* **1997**, *107*, 8554.

(18) (a) Hopkins, A. G.; Brown, C. W. *J. Chem. Phys.* **1975**, *62*, 2511 (SO). (b) Bondybey, V. E.; English, J. H. *J. Mol. Spectrosc.* **1985**, *109*, 221 (SO_3).

(19) Chen, L. S.; Lu, C. I.; Lee, Y. P. *J. Chem. Phys.* **1996**, *105*, 9454 (SOO).

(20) (a) Forney, D.; Kellogg, C. B.; Thompson, W. E.; Jacox, M. E. *J. Chem. Phys.* **2000**, *113*, 86, and references therein (SO_2^-). (b) Stanbury, D. M.; Holme, T. A.; Kafafi, Margrave, J. L. *Chem. Phys. Lett.* **1986**, *129*, 181(SO_3^-).

(21) Chertihin, G. V.; Bare, W. D.; Andrews, L. *J. Chem. Phys.* **1997**, *107*, 2798 (Cr + O_2).

(22) Bare, W. D.; Souter, P. F.; Andrews, L. *J. Phys. Chem. A* **1998**, *102*, 8279 (Mo, W + O_2).

(23) Zhou, M.; Andrews, L. *J. Chem. Phys.* **1999**, *111*, 4230 (Cr, Mo, W + O_2 in neon).

(24) Jacox, M. E. *Chem. Phys.* **1994**, *189*, 149.

(25) Liang, B.; Andrews, L. *J. Phys. Chem. A* **2002**, *106*, 6945 (Cr, Mo, W + S_2).

(26) (a) Scott, A. P.; Radom, L. *J. Phys. Chem.* **1996**, *100*, 16502. (b) Andersson, M. P.; Uvdal, P. L. *J. Phys. Chem. A* **2005**, *109*, 2937.

(27) Andrews, L.; Cho, H.-G. *Organometallics* **2006**, *25*, 4040, and references therein.

(28) Lyon, J. T.; Cho, H.-G.; Andrews, L. *Organometallics* **2007**, *26*, 6373 (Gr 6 + CHX_3, CX_4).

(29) Zhou, M. F.; Andrews, L.; Bauschlicher, C. W., Jr. *Chem. Rev.* **2001**, *101*, 1931, and references therein.

(30) Wang, X.; Andrews, L. *J. Phys. Chem. A* **2006**, *110*, 10409 (Gr 6 + H_2O_2).

(31) Gutsev, G. L.; Andrews, L.; Bauschlicher, C. W., Jr. *Theor. Chem. Acc.* **2003**, *109*, 298.

JP9033408